

# Evaluation of Encoded MU-MISO-OFDM Systems in TDD Mode with Non-ideal Channel Reciprocity

Mark Petermann, Dirk Wübben and Karl-Dirk Kammeyer

Department of Communications Engineering

University of Bremen, 28359 Bremen, Germany

Email: {petermann, wuebben, kammeyer}@ant.uni-bremen.de

**Abstract**—In multi-user orthogonal frequency division multiplexing (MU-OFDM) systems operating in time division duplex (TDD) mode downlink pre-equalization can be applied relying on channel state information (CSI) from the uplink direction. Unfortunately, the prerequisite of channel reciprocity is usually not fulfilled due to non-reciprocal transceivers. Hence, this paper deals with a comparison of robust pre-equalization schemes and a calibration approach to enhance the necessary uplink-downlink link equivalence for MU-MISO-OFDM systems applying linear and non-linear pre-equalization techniques and strong forward error correction (FEC). Performance evaluations concerning coded bit error rate results show that robust pre-equalizers exclusively improve the performance in moderate non-reciprocity conditions. In contrast, only calibration helps in dealing with severe transceiver mismatch.

## I. INTRODUCTION

The application of OFDM in wireless communication systems offers an easy equalization of frequency-selective channels [1]. In combination with multiple antennas at the base station these systems provide an excellent means for space-division multiple access (SDMA) schemes per subcarrier for decentralized non-cooperative mobile stations [2]. In TDD mode a prerequisite for exploitation of the uplink (UL) channel estimate as the basis for the pre-equalization filter matrices is channel reciprocity. Then, the uplink channel state information (UL-CSI) estimate can be used if the transmission interval is short compared to the channel coherence time. Unfortunately, non-reciprocal transceivers annihilate the reciprocity condition due to their different front-end components in the transmit and receive chains. Hence, they cause gain and phase mismatches of the resulting pre-equalization weights and multiuser interference is introduced into the system [3].

If the estimated CSI of the up- and downlink (DL) channels can be provided at the transmitter during a special calibration phase or with the help of so-called analog feedback [4], the reciprocity parameters of the existing transmit and receive filters can be estimated using, e.g., a total least squares (TLS) approach [5], [6]. Another way is a robust dimensioning of the transmit filters [2], [6]–[8]. The known mean deviation from channel reciprocity can be included in the minimum mean square error (MMSE) filter design. In addition, improvements in terms of bit and frame error rates (BER/FER) compared to linear schemes can be achieved by introducing

non-linear precoding strategies like Tomlinson-Harashima Precoding (THP) [7], [9], [10]. Together with strong forward error correction (FEC) these systems are simultaneously able to achieve good error rate performance and to move the major complexity from the mobile terminals to the base station.

In this paper, a systematic analysis of multi-user multiple-input single-output (MISO) OFDM systems applying linear and non-linear pre-equalization in combination with channel coding is presented, while an imperfect base station transceiver calibration in a TDD scenario is experienced. Additionally, robust MMSE schemes are compared with a simple online calibration approach.

The remainder of the paper is organized as follows. In Sec. II the system and the applied extended channel model are described. Subsequently, in Sec. III the robust transmit pre-equalization filter designs for the linear and non-linear cases are stated. The relative calibration approach is reflected in Sec. IV and simulation results for different pre-equalization and coding schemes are shown in Sec. V. Finally, a conclusion and an outlook are given in Sec. VI.

## II. EXTENDED SYSTEM MODEL

A DL scenario of a system with one single base station equipped with  $N_B$  antennas and  $N_M \leq N_B$  decentralized single-antenna mobile stations (MS) using OFDM with  $N_C$  subcarriers is considered. The vector of transmit symbols in frequency-domain is obtained by preprocessing the  $M$ -QAM symbol vector  $\mathbf{d} = [d_1, \dots, d_{N_B}]^T$  with unit variance by applying pre-equalization. To satisfy a total power constraint of  $N_B$  at the BS, the transmit symbols are scaled to ensure unit gain after pre-equalization. At the mobile stations complex Gaussian i.i.d. noise samples with variance  $\sigma_n^2$  are added.

Fig. 1 shows the extended channel model including the transceiver paths proposed in [7], [11], where  $\mathbf{a}_{[B/M],[i/j]}$  and  $\mathbf{b}_{[B/M],[i/j]}$  are auxiliary vectors for the transmit and receive signals in UL and DL direction, respectively. The  $i$ -th transmit and  $j$ -th receive antenna front-ends in the downlink, e.g., are modeled as two-port devices using a scattering matrix description [11]–[13],

$$\mathbf{T}_{[B/M],i} = \begin{bmatrix} 0 & 0 \\ \alpha_{T[B/M],i} & \gamma_{T[B/M],i} \end{bmatrix} \quad (1)$$

and

$$\mathbf{R}_{[B/M],j} = \begin{bmatrix} 0 & \alpha_{R[B/M],j} \\ 0 & \gamma_{R[B/M],j} \end{bmatrix}, \quad (2)$$

This work was supported in part by the German Research Foundation (DFG) under grant Ka841-21/1.

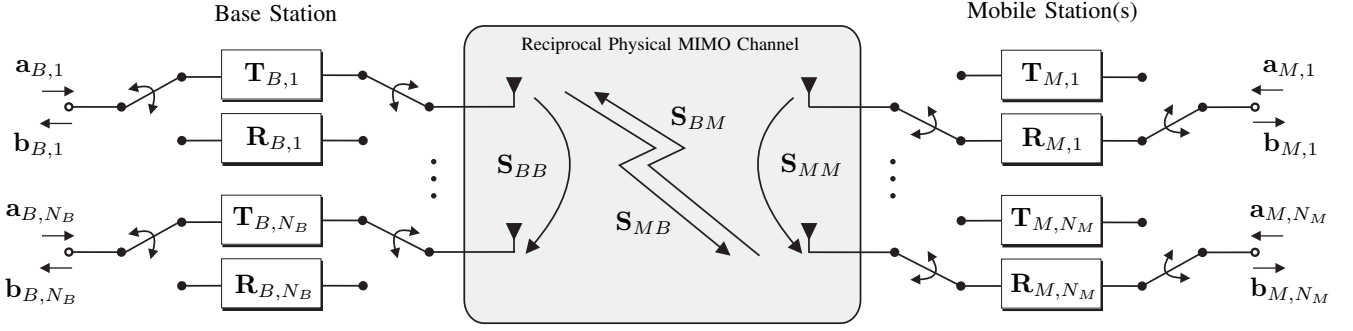


Fig. 1. Extended channel model using S-parameter description with BS and MS in downlink mode

with complex gain factors  $\alpha_{[T/R][B/M],[i/j]}$  and input/output reflection coefficients  $\gamma_{[T/R][B/M],[i,j]}$ . These factors are arranged in diagonal matrices, e.g.,

$$\mathbf{A}_{[T/R]B} = \text{diag}\{\alpha_{[T/R]B,1}, \dots, \alpha_{[T/R]B,N_B}\} \quad (3a)$$

$$\mathbf{\Gamma}_{[T/R]B} = \text{diag}\{\gamma_{[T/R]B,1}, \dots, \gamma_{[T/R]B,N_B}\}. \quad (3b)$$

Each gain factor, e.g.,  $\alpha_{[T/R]B,i} = 1 + \delta_{[T/R]B,i}$  is assumed to be slightly mismatched. Here, the statistically independent error terms  $\delta_{[T/R]B,i}$  are zero mean complex Gaussian random variables with variance  $\sigma_\delta^2$  [7]. These factors are expected to change very slowly in time compared to the duplex phase and assumed to be equal per antenna on all subcarriers  $k$ .

Thus, the effective down- and uplink matrices in frequency-domain on subcarrier  $k$  using the scattering matrix approach can be written as

$$\mathbf{H}(k) = \mathbf{A}_{RM} \mathbf{W}_{RM} \mathbf{S}_{MB}(k) \mathbf{W}_{TB} \mathbf{A}_{TB}, \quad (4)$$

and

$$\mathbf{G}(k) = \mathbf{A}_{TM} \mathbf{W}_{TM}^T \mathbf{S}_{MB}(k) \mathbf{W}_{RB}^T \mathbf{A}_{RB} \quad (5)$$

respectively. In (5) and (4) the matrices

$$\mathbf{W}_{T[B/M]} = (\mathbf{I}_{N_{[B/M]}} - \mathbf{\Gamma}_{T[B/M]} \mathbf{S}_{[BB/MM]})^{-1} \quad (6a)$$

$$\mathbf{W}_{R[B/M]} = (\mathbf{I}_{N_{[B/M]}} - \mathbf{S}_{[BB/MM]} \mathbf{\Gamma}_{R[B/M]})^{-1} \quad (6b)$$

describe the coupling and reflection at the transceivers. However, coupling and reflection effects can be neglected here as transceivers have to be well-matched to at least approximate channel reciprocity in a properly working system [7]. Then, with  $\mathbf{\Gamma}_{[\cdot]} \approx \mathbf{0}$  and  $\mathbf{S}_{[BB/MM]}$  close to the all zero matrix,  $\mathbf{W}_{T[B/M]}$  and  $\mathbf{W}_{R[B/M]}$  become identity matrices. In [11] the assumption of neglecting the influence of the reflection coefficients in (3b) is justified by means of realistic matching. Finally, reasoning that during DL transmission the uplink chain at the mobile terminals is disconnected, meaning that  $\mathbf{a}_{M,j} = \mathbf{0}$  in Fig. 1, the scattering matrix  $\mathbf{S}_{MB}(k)$  can directly be replaced by the "extrinsic" downlink physical MIMO channel matrix  $\mathbf{H}_{FD}(k)$  [12]. The channel matrix  $\mathbf{H}_{FD}(k)$  in frequency-domain results from the frequency-selective time-domain channel matrix  $\mathbf{H}_{TD}(\ell) \in \mathbb{C}^{N_M \times N_B}$ ,  $0 \leq \ell \leq L_F - 1$ , whose elements are i.i.d. complex Gaussian distributed. Here,  $L_F$  denotes the number of uncorrelated equal power channel taps.

### III. PRE-EQUALIZATION

#### A. Linear MMSE Pre-Equalization

If linear pre-equalization is applied the receive signal  $\mathbf{y}(k) = [y_1(k), \dots, y_{N_M}(k)]^T$  on subcarrier  $k$  stacking all mobile stations reads

$$\mathbf{y}(k) = \beta(k) \mathbf{H}(k) \mathbf{F}(k) \mathbf{d}(k) + \mathbf{n}(k), \quad (7)$$

where  $\mathbf{d}(k) \in \mathbb{C}^{N_M \times 1}$  is the data vector to be transmitted to the  $N_M$  mobile stations. The pre-equalization matrix  $\mathbf{F}(k) \in \mathbb{C}^{N_B \times N_M}$  in the MMSE case is determined using the uplink channel matrix  $\mathbf{G}(k)$  such that

$$\mathbf{F}_{\text{MMSE}}(k) = \mathbf{G}^H(k) (\mathbf{G}(k) \mathbf{G}^H(k) + \sigma_n^2 \mathbf{I}_{N_M})^{-1} \quad (8)$$

holds. Here, the same noise power  $\sigma_n^2$  on all subcarriers and all MS is assumed. The scalar

$$\beta(k) = \sqrt{\frac{N_B}{\text{tr}\{\mathbf{F}(k)^H \mathbf{F}(k)\}}} \quad (9)$$

is chosen such that the total sum power constraint per subcarrier is fulfilled. For sake of brevity we drop the subcarrier index  $k$  for the remainder of this section.

As shown in [7] with the assumptions of perfect decoupling and the fact that the gain factors at the mobile terminals can be set to one (i.e.  $\delta_{[T/R]M,j} = 0$ ) due to compensation, e.g., by pilot aided channel estimation, the effective downlink matrix in (4) depends on the term  $\mathbf{A}_{RB}^{-1} \mathbf{A}_{TB}$  (cf. (17)), which in case of  $\mathbf{A}_{RB} \neq \mathbf{A}_{TB}$  leads to interference caused by non-reciprocal transceivers. This can be illustrated by evaluating the receive signals using (8), which yields (10a)-(10c). Now, if  $|\delta_{[T/R]B,i}| \ll 1$  the term  $\mathbf{A}_{RB}^{-1} \mathbf{A}_{TB}$  can be approximated by  $\mathbf{I}_{N_B} + \mathbf{\Delta}$ . Then, the estimated receive data is

$$\tilde{\mathbf{d}} = \beta^{-1} \mathbf{y} = (\mathbf{G} + \mathbf{G} \mathbf{\Delta}) \mathbf{F} \mathbf{d} + \beta^{-1} \mathbf{n}, \quad (11)$$

with  $\mathbf{\Phi}_{\mathbf{\Delta}} = \mathbf{E}\{\mathbf{\Delta} \mathbf{\Delta}^H\} = 2 \cdot \sigma_\delta^2 \mathbf{I}_{N_B}$  being the covariance matrix of the reciprocity error. With (11) a robust MMSE pre-equalizer design with respect to non-reciprocal transceivers can be derived following the principles in [7], [8] such that

$$\mathbf{F}_{\text{rMMSE}} = (\mathbf{G}^H \mathbf{G} + \sigma_n^2 \mathbf{I}_{N_B} + \text{dg}\{\mathbf{\Phi}_{\mathbf{\Delta}} \mathbf{G}^H \mathbf{G}\})^{-1} \mathbf{G}^H. \quad (12)$$

Here,  $\text{dg}\{\cdot\} \hat{=} \text{diag}\{\text{diag}^{-1}\{\cdot\}\}$  sets all off-diagonals of a matrix to zero [7]. With (10a)-(10c) and similar considerations

$$\begin{aligned}\tilde{\mathbf{d}} = \beta^{-1}\mathbf{y} &= \mathbf{H}\mathbf{G}^H (\mathbf{G}\mathbf{G}^H + \sigma_n^2\mathbf{I}_{N_M})^{-1} \mathbf{d} + \beta^{-1}\mathbf{n} \\ &= \underbrace{\mathbf{A}_{RM} \left( \mathbf{I}_{N_M} + \sigma_n^2 (\mathbf{H}_{FD}\mathbf{A}_{RB}\mathbf{A}_{RB}^H\mathbf{H}_{FD}^H\mathbf{A}_{TM}^H\mathbf{A}_{TM})^{-1} \right)^{-1} \mathbf{A}_{TM}^{-1}\mathbf{d}}_{\text{useful signal}}\end{aligned}\quad (10a)$$

$$+ \underbrace{\mathbf{A}_{RM}\mathbf{H}_{FD}(\mathbf{A}_{TB} - \mathbf{A}_{RB})\mathbf{A}_{RB}^H\mathbf{H}_{FD}^H \left( \mathbf{H}_{FD}\mathbf{A}_{RB}\mathbf{A}_{RB}^H\mathbf{H}_{FD}^H + \sigma_n^2 (\mathbf{A}_{TM}^H\mathbf{A}_{TM})^{-1} \right)^{-1} \mathbf{A}_{TM}^{-1}\mathbf{d}}_{\text{interference due to TX / RX mismatch}}\quad (10b)$$

$$+ \underbrace{\beta^{-1}\mathbf{A}_{RM}\mathbf{n}}_{\text{scaled noise}}\quad (10c)$$

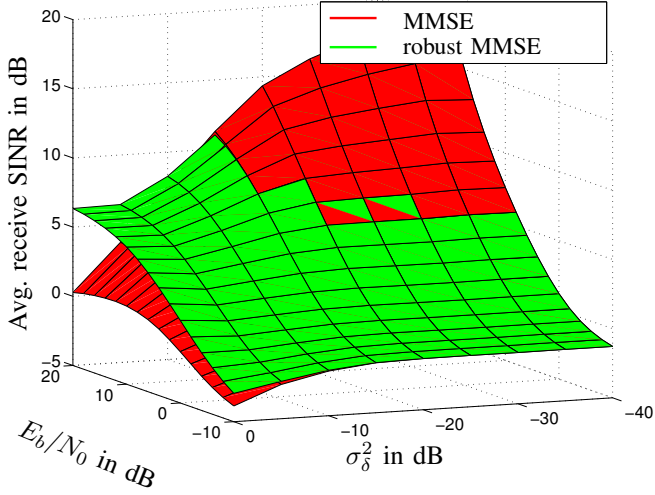


Fig. 2. Average receive SINR for all users per subcarrier in an uncoded  $N_B = N_M = 4$  system and 16-QAM with a common and a robust MMSE filter design versus the reciprocity parameter  $\sigma_\delta^2$  and the  $E_b/N_0$ -ratio

for the robust solution in (12) the average receive signal-to-interference plus noise-ratio (SINR) per subcarrier can be analyzed numerically with respect to different reciprocity conditions  $\sigma_\delta^2$  and the ratio  $E_b/N_0 = N_M/(\log_2(M)\sigma_n^2)$ . The results for an uncoded 16-QAM modulation are shown in Fig. 2. There, the superiority of the robust approach can be seen especially for large reciprocity errors and high transmit powers. This motivates the combination with strong FEC, as with the application of channel coding the operation point concerning the  $E_b/N_0$  ratio is at low to moderate transmit powers. Hence, the gain of the robust solution might vanish and the complexity of the filter matrix calculation can be reduced.

### B. Non-Linear MMSE Tomlinson-Harashima Precoding

Tomlinson-Harashima Precoding (THP) is a non-linear structure for modulo receivers and is the transmit equivalent of a decision feedback equalization (DFE) structure at the receiver [2]. It is applied at the transmitter to avoid error propagation stemming from previously wrong decided data in the DFE at the cost of necessary transmit CSI at the base station. The transmit structure is exemplarily shown in Fig. 3.

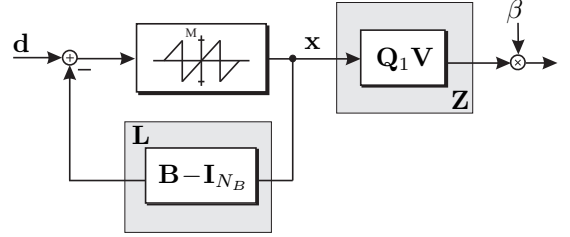


Fig. 3. Structure of the Tomlinson-Harashima precoder

It consists of a feedforward filter matrix  $\mathbf{Z}$  to obtain causality and a triangular feedback filter matrix  $\mathbf{L}$  to presubtract the interference caused by previously precoded data from other users. Both matrices in the MMSE case can be calculated with the extended channel matrix

$$\underline{\mathbf{G}} = \left[ \mathbf{G}, \sqrt{\sigma_n^2}\mathbf{I}_{N_M} + \text{dg}\{\Phi_\Delta\mathbf{G}^H\mathbf{G}\} \right], \quad (13)$$

where the last summand is exclusively used for the robust THP-MMSE approach. By applying a QR decomposition of  $\underline{\mathbf{G}}^H$  such that

$$\underline{\mathbf{G}}^H = \mathbf{Q}\mathbf{R} = [\mathbf{Q}_1^T, \mathbf{Q}_2^T]^T \mathbf{V}\mathbf{R}' \quad (14)$$

the matrix  $\mathbf{Q}_1 \in \mathbb{C}^{N_B \times N_B}$  and the diagonal matrix  $\mathbf{V} = \text{diag}\{r_{1,1}, \dots, r_{N_B, N_B}\}$  are obtained. The feedforward filter matrix is defined by  $\mathbf{Z} = \mathbf{Q}_1\mathbf{V}$ . Setting matrix  $\mathbf{B} = \text{LoT}\{\mathbf{G}\mathbf{Q}_1\mathbf{V}\}$ , where  $\text{LoT}\{\cdot\}$  picks the lower triangular part of a matrix and inserts ones on the main diagonal, the feedback filter matrix results in  $\mathbf{L} = \mathbf{B} - \mathbf{I}_{N_B}$ . The symbols at the input of the detector can then be described by

$$\tilde{\mathbf{d}} = \text{mod}_{2\sqrt{M}}\{\mathbf{B}\mathbf{x} + \beta^{-1}\mathbf{n}\}, \quad (15)$$

where  $\text{mod}_\lambda\{x\} = x - \lfloor \frac{x}{\lambda} + \frac{1}{2} \rfloor \lambda$  defines the modulo-operator concerning the Voronoi regions in the extended symbol constellation [7]. To fulfill the power constraint the scalar  $\beta$  has to be adjusted accordingly such that the

$$\beta = \sqrt{\frac{N_B}{\text{tr}\{\mathbf{Q}_1\mathbf{V}\mathbf{V}^H\mathbf{Q}_1^H\}}}. \quad (16)$$

#### IV. DOWNLINK CHANNEL CALIBRATION

Instead of a robust filter design a calibration of the system can be executed, provided that both the uplink and downlink CSI are available at the BS. For the purpose of estimating the reciprocity coefficients  $\alpha_{[T/R],B,i}$  it is assumed that the uplink and downlink CSI at the BS may both be disturbed by noise due to the assumption of imperfect channel estimation and erroneous analog feedback. Nevertheless, assuming perfect CSI during the derivation and  $\mathbf{W}_{T[B/M]} = \mathbf{W}_{R[B/M]} = \mathbf{I}_{N_{[B/M]}}$  equation (4) can be rewritten using (5) as

$$\mathbf{H}(k) = \underbrace{\mathbf{A}_{RM} \mathbf{A}_{TM}^{-T}}_{\mathbf{C}_M} \mathbf{G}(k) \underbrace{\mathbf{A}_{RB}^{-T} \mathbf{A}_{TB}}_{\mathbf{C}_B}. \quad (17)$$

With definition of the vectors  $\mathbf{c}_B \triangleq \text{diag}^{-1}\{\mathbf{C}_B^{-1}\}$  and  $\mathbf{c}_M \triangleq \text{diag}^{-1}\{\mathbf{C}_M^T\}$  equation (17) can be reformulated with  $\mathbf{c} \triangleq [\mathbf{c}_B^T \mathbf{c}_M^T]^T$  to

$$\mathbf{E}\mathbf{c} = \mathbf{0}_{N_B N_M \times 1}, \quad (18)$$

where  $\mathbf{E}$  is composed of the the rows of  $\mathbf{G}(k)$  and  $\mathbf{H}(k)$  (cf. [5]) such that

$$\mathbf{E} = [\mathbf{E}_1^T, \dots, \mathbf{E}_K^T]^T \quad (19a)$$

with

$$\mathbf{E}_k = \begin{bmatrix} \text{diag}\{\mathbf{h}^{(1)}(k)\} & -\mathbf{g}^{(1)T}(k) & \mathbf{0} \\ \vdots & \ddots & \\ \text{diag}\{\mathbf{h}^{(N_M)}(k)\} & \mathbf{0} & -\mathbf{g}^{(N_M)T}(k) \end{bmatrix}. \quad (19b)$$

Here,  $K$  defines the number of subcarriers used for calibration. A number  $K > 1$  has the benefit of increasing the number of coefficients compared to the number of unknowns in  $\mathbf{c}$ .

Following [5], [6], (18) defines a special case of a total least squares (TLS) problem [14], where

$$\underset{\Delta \mathbf{E}}{\text{minimize}} \quad \|\Delta \mathbf{E}\|_F \quad (20a)$$

$$\text{such that} \quad (\mathbf{E} + \Delta \mathbf{E})\mathbf{c} = \mathbf{0}_{N_B N_M \times 1} \quad (20b)$$

has to be solved. The goal is to find a perturbation matrix  $\Delta \mathbf{E}$  with minimum Frobenius norm that lowers the rank of  $\mathbf{E}$ , where  $\Delta \mathbf{E}$  is the correction term of the TLS optimization problem. This specific problem is valid for narrowband flat-fading as in OFDM on each subcarrier and sparse filter matrices (3a) [5].

The solution to (18) lies in the right null space of  $\mathbf{E}$  and can be computed with the singular value decomposition (SVD). In [14] the connection of the TLS solution to the SVD was shown. Then, if  $\mathbf{E} = \mathbf{U}\mathbf{\Sigma}\mathbf{V}^T$  depicts the SVD and matrix  $\mathbf{V} = [\mathbf{v}_1, \dots, \mathbf{v}_{N_B+N_M}]$  denotes the right singular vector space, the estimated solution to  $\mathbf{c}$  depends on the right singular vector corresponding to the smallest singular value in  $\mathbf{\Sigma}$  such that

$$\mathbf{c}_0 = -\frac{1}{v_{N_B+N_M, N_B+N_M}} \mathbf{v}_{N_B+N_M}. \quad (21)$$

Thus,  $\mathbf{c}$  can be fully determined (up to a scalar coefficient, which vanishes due to the reciprocal multiplication in (17)) if and only if  $v_{N_B+N_M, N_B+N_M} \neq 0$  holds [14], [15]. With  $\mathbf{c}_0$  the matrices  $\mathbf{G}(k)$  can be adjusted according to (17).

#### V. SIMULATION RESULTS

In this section bit error rate results versus  $E_b/N_0$  for different pre-equalization strategies in a coded  $N_B = N_M = 4$  multi-user MISO-OFDM scenario applying  $N_C = 256$  subcarriers and 16-QAM transmission are shown. The QAM soft output demapping is done via max-log approximation. For the applied channel coding either a half-rate 3GPP Turbo Code with additional sub-block interleaving [16] or a half-rate irregular low-density parity check (LDPC) code based on progressive edge growth construction [17], [18] with a regular column weight of three is used. For the turbo code the specified code rate is achieved via the 3GPP rate matching algorithm also given in [16]. The LDPC code is decoded via the sum-product algorithm with a maximum of 100 iterations. It is assumed that a codeword ranges over six OFDM symbols.  $E_b$  denotes the average energy per information bit arriving at the receiver, thus  $E_b/N_0 = N_M/(R_c \log_2(M)\sigma_n^2)$  holds, where  $R_c$  is the code rate of the applied channel code. The guard interval has a length of  $N_g = 6$ , which is equal to the length of the considered equal power Rayleigh channel taps  $L_F$  here. The channel is constant for one codeword but changes from codeword to codeword. For completeness, it has to be mentioned that the guard loss is also considered in the results.

The reference curve for linear zero-forcing (ZF) pre-equalization in Fig. 4, which is built via the pseudo-inverse  $\mathbf{G}^H(k) (\mathbf{G}(k)\mathbf{G}^H(k))^{-1}$ , shows a poor behavior even with strong turbo encoding. This indicates the inadequate application of linear ZF in a multi-user scenario for decentralized non-cooperative receivers if the user streams have to be encoded separately. This was done for all results and is also known as per-stream or per-layer coding.

The left-most solid line depicts the optimum achievable

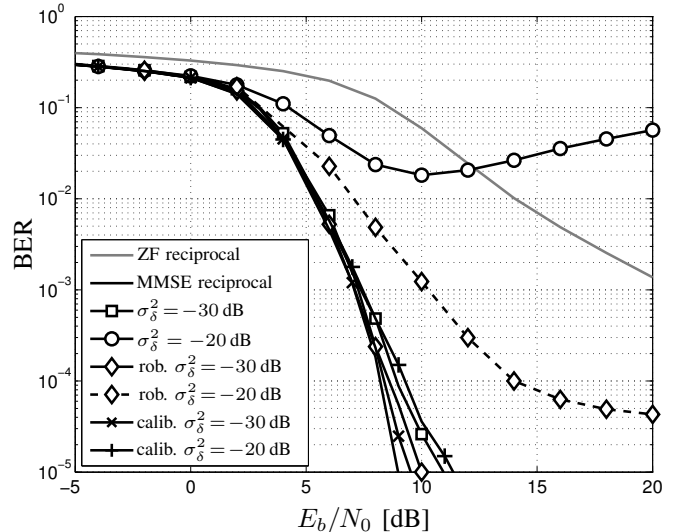


Fig. 4. BER versus  $E_b/N_0$  for a system with  $N_B = N_M = 4$ ,  $N_C = 256$  subcarriers and 16-QAM with linear pre-equalization and different reciprocity mismatch conditions - channel coding with a punctured half-rate 3GPP Turbo code

performance with a linear MMSE pre-equalizer and perfect reciprocity ( $\sigma_\delta^2 = 0$ ). With the turbo code a BER of  $10^{-4}$  can be achieved at 8 dB  $E_b/N_0$ . If the transceiver mismatch is  $\sigma_\delta^2 = -30$  dB the degradation is marginal with a loss of 1.5 dB at a low BER of  $10^{-4}$  compared to the perfect case. The strong encoding seems to be able to cope with a moderate mismatch for itself. An increase in the mismatch saturates the performance and ends up with an increasing BER at high SNR regions. This behavior can be explained with (10b), where the dependency of the interference from a reciprocity mismatch is inversely related to the noise power  $\sigma_n^2$ . Consequently, a low noise power results in large interference arising from the transceiver mismatch.

This behavior has to be avoided by means of robust MMSE pre-equalization or calibration procedures. Hence, in Fig. 4 the results for robust pre-equalization show an improvement of 1 dB at a BER of  $10^{-5}$  for the moderate transceiver mismatch of  $\sigma_\delta^2 = -30$  dB, while an increasing mismatch directly leads to an error floor even with a turbo code. Nevertheless, an increasing BER can be avoided. The calibration scheme with ordinary MMSE according to (8) and  $K = 1$  can cope with a large reciprocity mismatch but requiring extra DL-CSI at the base station. As a consequence of this, the increase of parameter  $K > 1$  is not justified for coded systems and frequency-flat front-end filter matrices as in (5) and (4) due to the small room for improvements in terms of BER and the comparably high complexity increase in the SVD. For a comparison of different  $K$ -parameters in the uncoded case the interested reader is referred to [6].

The results for Tomlinson-Harashima precoding and turbo coding in Fig. 5 show almost similar behavior. To analyze the encoded behavior the log-likelihood ratios (LLRs) for THP are required. Therefore, due to the modulo device and the resulting cyclic equivalent decision regions the likelihood values prior to the turbo and or LDPC decoder should be computed over an infinite sum. Nevertheless, the extended receive symbol constellation can be used for max-log approximation [19], [20]. It can be shown that at least two or three neighboring symbols are sufficient to approximate the infinite sum.

Firstly, applying non-linear precoding does not show any significant improvement for the MMSE filter design with perfect reciprocity, which substantiates the dominance of strong FEC and the need for a careful choice of the trade-off between channel coding and precoding. But it indicates an inherently higher robustness of THP against reciprocity errors, which can be seen for  $\sigma_\delta^2 = -20$  dB. Beyond that, the gain of THP-MMSE compared to THP applying the ZF solution is around 7 dB at a BER of  $10^{-4}$ . Considering the influence of non-reciprocity a moderate transceiver mismatch leads to a minor degradation of around 0.5 dB. A further increasing mismatch still leads to an error floor and the behavior mentioned above. The application of robust precoding only helps at large reciprocity mismatch, where a gap of 3 dB at a BER of  $10^{-4}$  remains. For small to moderate mismatch the robust solution gives minor improvements, a further improvement can be achieved with calibration, whereas the performance gain for

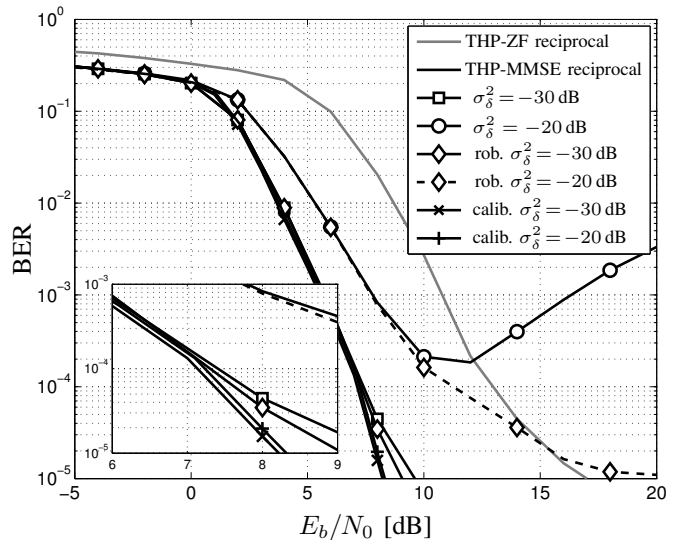


Fig. 5. BER versus  $E_b/N_0$  for a system with  $N_B = N_M = 4$ ,  $N_C = 256$  subcarriers and 16-QAM using Tomlinson-Harashima precoding and different reciprocity mismatch conditions - channel coding with a punctured half-rate 3GPP Turbo code

both schemes is in tenths of a dB and in BER regions, which are not of interest in real systems.

Fig. 6 and Fig. 7 show the equivalent results for the application of LDPC codes in MU-MISO-OFDM systems with linear and non-linear pre-equalization, respectively. First, the overall encoding performance is slightly worse, which is mainly due to the insufficient codeword length containing only 3072 information bits per user. Furthermore, with  $\sigma_\delta^2 = -20$  dB the BER again shows an error floor at high SNR for the robust scheme, while for a moderate non-reciprocity condition with  $\sigma_\delta^2 = -30$  dB the gain is around 0.75 dB at a BER of  $10^{-4}$ . In contrast, calibrating the system using  $K = 1$  subcarriers achieves the maximum performance of a reciprocal TDD system with MMSE pre-equalization.

Again, the LDPC code results for THP show the robustness of THP precoding. Even for a high reciprocity mismatch the loss at a BER of  $10^{-3}$  is only 3 dB compared to the perfect THP-MMSE case without any action against the error. Robust solutions avoid the error floor at high SNR and in high mismatch situations but in particular are not able to improve the performance at interesting operation points of  $10^{-3}$  BER.

## VI. CONCLUSION

In this contribution the influence of non-reciprocal transceivers at the base station in MU-MISO-OFDM systems with linear and non-linear pre-equalization, respectively, and strong forward error correction is investigated. Especially the ideas of robust MMSE and signal-space calibration approaches are compared in terms of BER results. The performance results for both linear and non-linear schemes show a superior behavior of the calibration in combination with an ordinary MMSE pre-equalization. Calibration allows for combating severe reciprocity mismatch while a robust MMSE approach

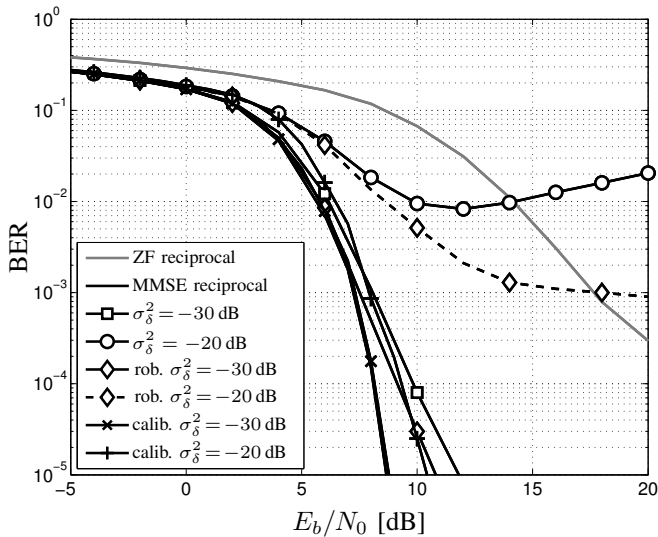


Fig. 6. BER versus  $E_b/N_0$  for a system with  $N_B = N_M = 4$ ,  $N_C = 256$  subcarriers and 16-QAM using linear pre-equalization and different reciprocity mismatch conditions - channel coding with a half-rate LDPC code

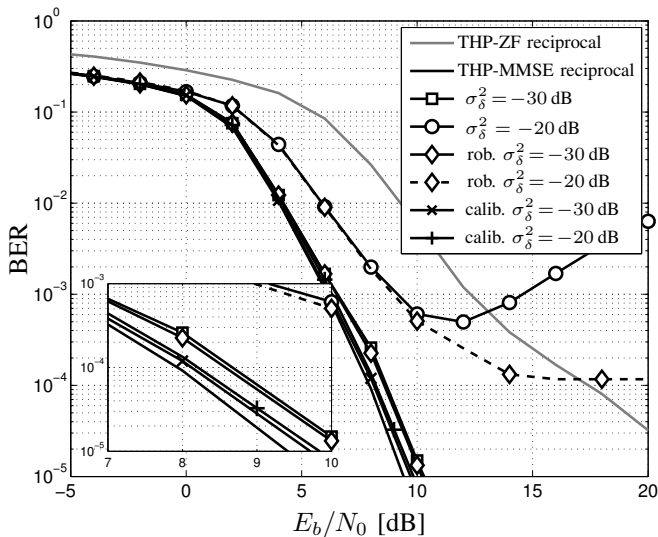


Fig. 7. BER versus  $E_b/N_0$  for a system with  $N_B = N_M = 4$ ,  $N_C = 256$  subcarriers and 16-QAM using Tomlinson-Harashima pre-equalization and different reciprocity mismatch conditions - channel coding with a half-rate LDPC code

can only handle moderate transceiver mismatches due to the approximation made in (11). This indicates that strong FEC in combination with robust pre-equalization does not suffice to fully exploit UL-CSI for downlink pre-equalization. In order to decrease the requirements on transceiver front-end components calibration is inevitable to cope with large transmit and receive chain mismatches in TDD systems. In contrast, for decreasing reciprocity mismatch the application of less complex robust pre-equalizer solutions can be preferred as results for 16-QAM modulation revealed. This tendency is much more distinctive with powerful precoding schemes as an inherently higher robustness of THP against imperfect link equivalence in TDD systems compared to linear pre-equalization schemes was

observed. Consequently, in the future the influence of non-reciprocal transceivers should not be disregarded in the development of high-rate adaptive communication systems. For further research, the influence of vector precoding, frequency-selective front-end filter descriptions and less complex calibration approaches are of great interest.

## REFERENCES

- [1] J. A. C. Bingham, "Multicarrier modulation for data transmission: An idea whose time has come," *IEEE Commun. Mag.*, vol. 28, pp. 5–14, May 1990.
- [2] C. Windpassinger, R. F. H. Fischer, T. Vencel, and J. B. Huber, "Precoding in multi-antenna and multi-user communications," *IEEE Trans. Wireless Commun.*, vol. 3, no. 4, pp. 1305–1316, Jul. 2004.
- [3] A. Bourdoux, B. Come, and N. Khaled, "Non-reciprocal transceivers in OFDM/SDMA systems: Impact and mitigation," in *Radio and Wireless Conference (RAWCON)*, Boston, MA, USA, Aug. 2003, pp. 183–186.
- [4] T. L. Marzetta and B. M. Hochwald, "Fast transfer of channel state information in wireless systems," *IEEE Trans. Signal Process.*, vol. 54, no. 4, pp. 1268–1278, Apr. 2006.
- [5] M. Guillaud, "Transmission and channel modeling techniques for multiple-antenna communication systems," PhD thesis, Ecole Nationale Supérieure des Telecommunications, Paris, France, Jul. 2005.
- [6] M. Petermann, D. Wübben, and K. D. Kammeyer, "Calibration of non-reciprocal transceivers for linearly pre-equalized MU-MISO-OFDM systems in TDD mode," in *Proc. International OFDM-Workshop (InOWo)*, Hamburg, Germany, Sep. 2009, pp. 53–57.
- [7] R. Habendorf and G. Fettweis, "Pre-equalization for TDD systems with imperfect transceiver calibration," in *IEEE Proc. Vehicular Technology Conference (VTC), Spring*, Marina Bay, Singapore, May 2008.
- [8] M. Joham, K. Kusume, M. Gzara, W. Utschick, and J. A. Nossek, "Transmit wiener filter for the downlink of TDD DS-CDMA systems," in *Proc. IEEE Int. Symp. on Spread Spectrum Techniques and Applications (ISSSTA)*, vol. 1, Prague, Czech Rep., Sep. 2002, pp. 9–13.
- [9] M. Tomlinson, "New automatic equaliser employing modulo arithmetic," *IEE Electronics Letters*, vol. 7, no. 5, pp. 138–139, Mar. 1971.
- [10] H. Harashima and H. Miyakawa, "Matched-transmission technique for channels with intersymbol interference," *IEEE Trans. Commun.*, vol. COM-20, pp. 774–780, Aug. 1972.
- [11] L. Brühl, C. Degen, W. Keusgen, B. Rembold, and C. M. Walke, "Investigation of front-end requirements for MIMO-systems using downlink pre-distortion," in *European Personal Mobile Communications Conference (EPMCC)*, Glasgow, Scotland, Apr. 2003.
- [12] W. Keusgen, "Antennenkonfiguration und Kalibrierungskonzepte für die Realisierung reziproker Mehrantennensysteme," PhD thesis (in German), RWTH Aachen, Germany, Oct. 2005.
- [13] C. Waldschmidt, S. Schulteis, and W. Wiesbeck, "Complete RF system model for analysis of compact MIMO arrays," *IEEE Trans. Commun. Technol.*, vol. 53, no. 3, pp. 579–586, May 2004.
- [14] G. H. Golub and C. F. V. Loan, "An analysis of the total least squares problem," *SIAM Journal on Numerical Analysis*, vol. 17, no. 6, pp. 883–893, Dec. 1980.
- [15] M. Guillaud, D. T. M. Slock, and R. Knopp, "A practical method for wireless channel reciprocity exploitation through relative calibration," in *International Symposium on Signal Processing and its Applications (ISSPA)*, Sydney, Australia, Aug. 2005.
- [16] 3GPP TSG RAN, "E-UTRA; Multiplexing and Channel Coding (Release 8)," 3GPP, Tech. Rep. 36.212 V8.7.0, May 2009.
- [17] X. Y. Hu, E. Eleftheriou, and D. M. Arnold, "Regular and irregular progressive edge growth tanner graphs," *IEEE Trans. Inf. Theory*, vol. 51, pp. 386–398, Jan. 2005.
- [18] T. J. Richardson, M. A. Shokrollahi, and R. L. Urbanke, "Design of capacity-approaching irregular low-density parity-check codes," *IEEE Trans. Inf. Theory*, vol. 47, pp. 619–637, Feb. 2001.
- [19] C. B. Peel, B. M. Hochwald, and A. L. Swindlehurst, "A vector-perturbation technique for near-capacity multi-antenna multiuser communication part ii: Perturbation," *IEEE Trans. Commun.*, vol. 53, no. 1, pp. 203–203, Jan. 2005.
- [20] R. Habendorf and G. Fettweis, "Nonlinear predistortion for OFDM SDMA systems," in *IEEE Workshop on Signal Processing Advances in Wireless Communications (SPAWC)*, Cannes, France, Jul. 2006.